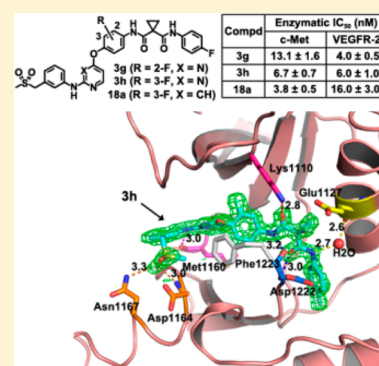


Discovery of Anilinyrimidines as Dual Inhibitors of c-Met and VEGFR-2: Synthesis, SAR, and Cellular Activity

Zhengsheng Zhan,^{†,||} Jing Ai,^{‡,||} Qiufeng Liu,^{§,||} Yinchun Ji,[‡] Tiantian Chen,[§] Yechun Xu,^{*,§} Meiyu Geng,^{*,‡} and Wenhui Duan^{*,†}[†]Department of Medicinal Chemistry, [‡]Division of Antitumor Pharmacology, and [§]Drug Discovery and Design Center, State Key Laboratory of Drug Research, Shanghai Institute of Materia Medica, Chinese Academy of Sciences, 555 Zu Chong Zhi Road, Shanghai 201203, China

Supporting Information

ABSTRACT: Both c-Met and VEGFR-2 are important targets for cancer therapies. Here we report a series of potent dual c-Met and VEGFR-2 inhibitors bearing an anilinyrimidine scaffold. Two novel synthetic protocols were employed for rapid analoguing of the designed molecules for structure–activity relationship (SAR) exploration. Some analogues displayed nanomolar potency against c-Met and VEGFR-2 at enzymatic level. Privileged compounds **3a**, **3b**, **3g**, **3h**, and **18a** exhibited potent antiproliferative effect against c-Met additive cell lines with IC₅₀ values ranged from 0.33 to 1.7 μM. In addition, a cocrystal structure of c-Met in complex with **3h** has been determined, which reveals the binding mode of c-Met to its inhibitor and helps to interpret the SAR of the analogues.



KEYWORDS: Anilinyrimidine, dual inhibitor, c-Met, SAR, VEGFR-2

The receptor tyrosine kinase c-Met and its natural ligand hepatocyte growth factor (HGF) generate the c-Met signaling, which promotes the invasive growth during embryonic development, wound healing, and oncogenesis.¹ Aberrant expression of c-Met/HGF axis has been detected in a variety of solid tumors.^{2–5} VEGFR-2 or KDR (kinase insert domain receptor), a member of vascular endothelial growth factor receptors (VEGFRs), also belongs to receptor tyrosine kinase family. Its activation by vascular endothelial growth factor (VEGF⁰) promotes several key processes required for forming new blood vessels.^{6,7}

c-Met has been shown to synergistically collaborate with VEGFR-2, resulting in promoting angiogenesis of development and progression of various human cancers.^{8–10} Therefore, molecules that simultaneously inhibit c-Met and VEGFR-2 may be superior to either c-Met-selective or VEGFR-2-selective inhibitor as they can interrupt multiple signaling pathways involved in tumor angiogenesis, proliferation, and metastasis.¹¹

Cabozantinib (**1** in Figure 1), an approved drug for the treatment of medullary thyroid cancer, is a highly potent c-Met and VEGFR-2 inhibitor.^{12,13} A similar compound, dianilinyrimidine urea **2**, was reported only as a potent VEGFR-2 inhibitor with an enzymatic IC₅₀ of 18 nM.¹⁴ The difference in the biological profiles of **1** and **2** implied that the cyclopropane-1,1-dicarboxamide moiety might be important for the high inhibition of both c-Met and VEGFR-2 of cabozantinib. On the basis of this assumption, we first designed and synthesized compound **3a**, which was a hybrid structure containing both

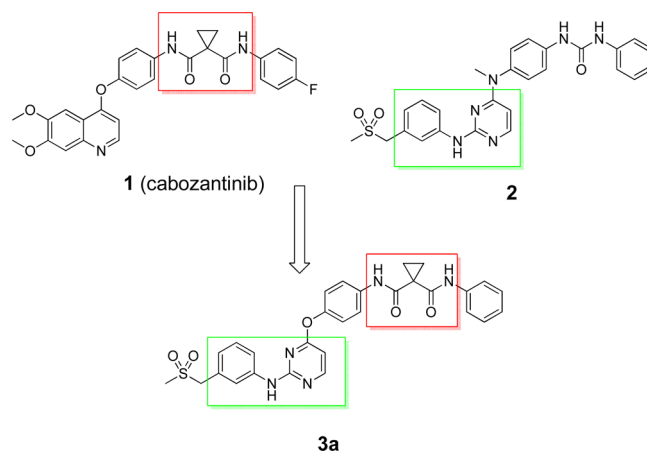


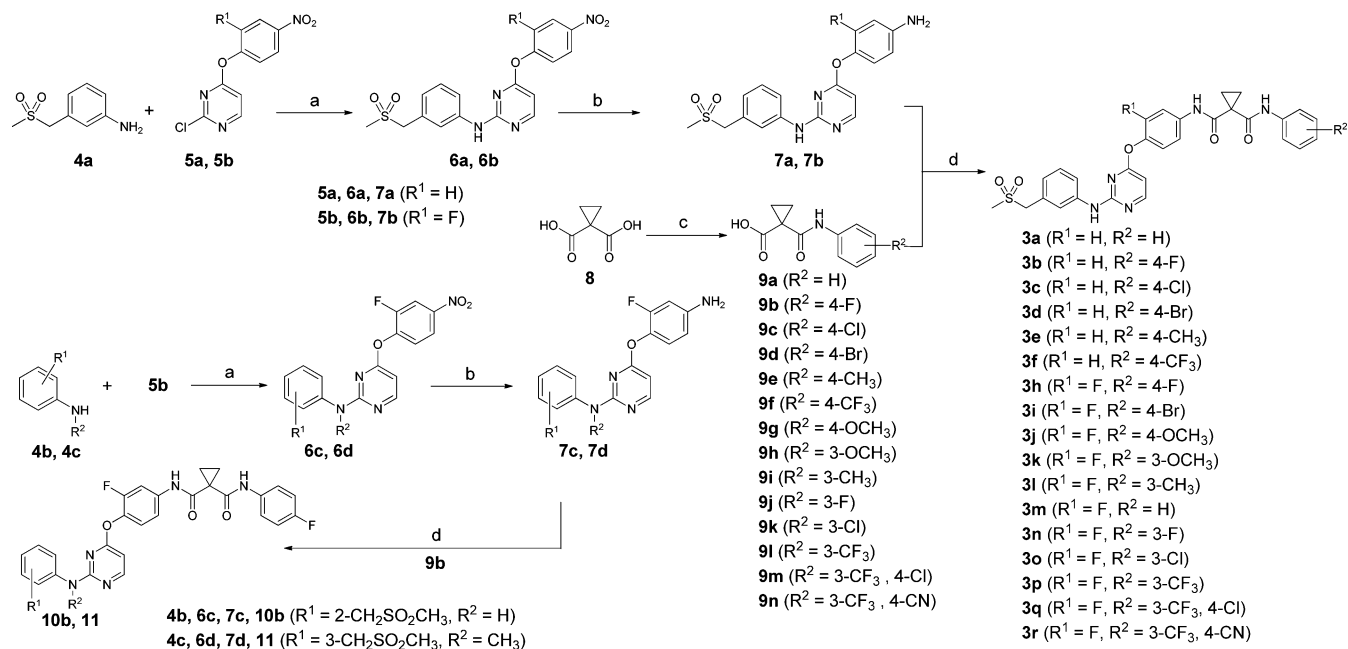
Figure 1. Design of the anilinyrimidine **3a**.

the cyclopropane-1,1-dicarboxamide moiety of cabozantinib and the anilinyrimidine core structure of **2** (Figure 1). As expected, compound **3a** potently inhibited both c-Met and VEGFR-2 with enzymatic IC₅₀ values of 8.8 and 16 nM, respectively. Encouraged by this promising result, we prepared

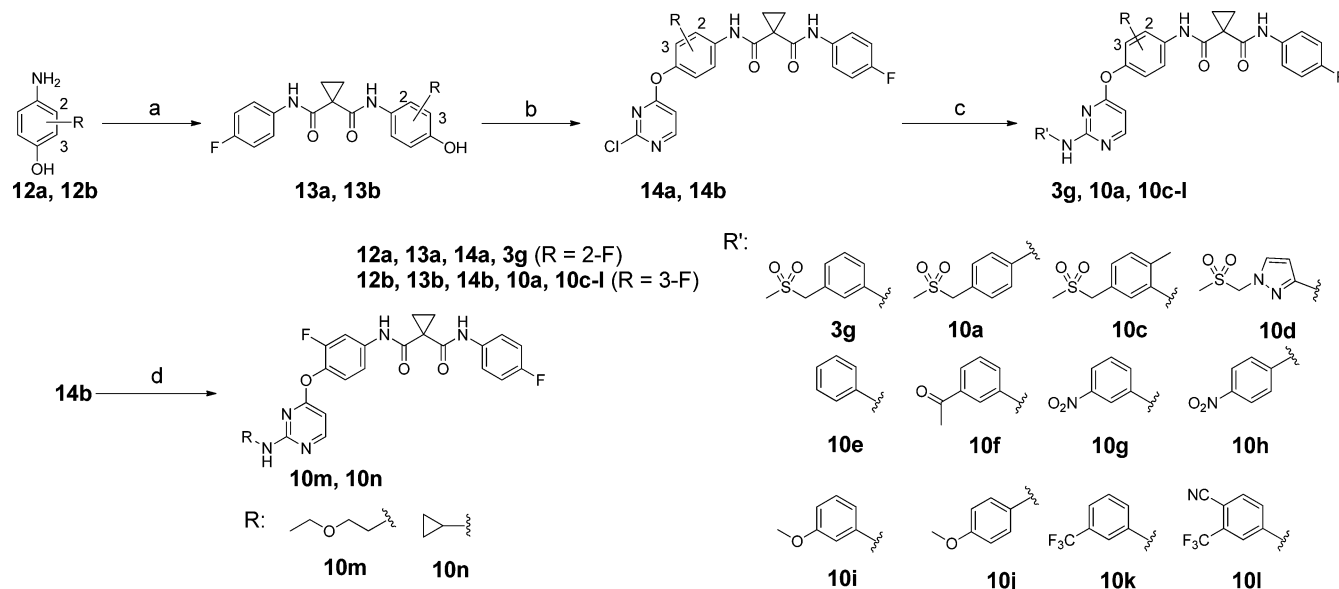
Received: February 10, 2014

Accepted: March 26, 2014

Published: March 26, 2014

Scheme 1. Synthesis of Compounds 3a–f, 3h–r, 10b, and 11^a

^aReagents and conditions: (a) *p*-toluene sulfonic acid monohydrate, DMF, 90 °C for **6a, 6b**, and **6d**/microwave at 80 °C for **6c**; (b) Fe, NH₄Cl, EtOH/H₂O, reflux; (c) SOCl₂, Et₃N, THF, then aniline or substituted aniline; (d) EDCl, DMF.

Scheme 2. Synthesis of Compounds 3g, 10a, and 10c–n^a

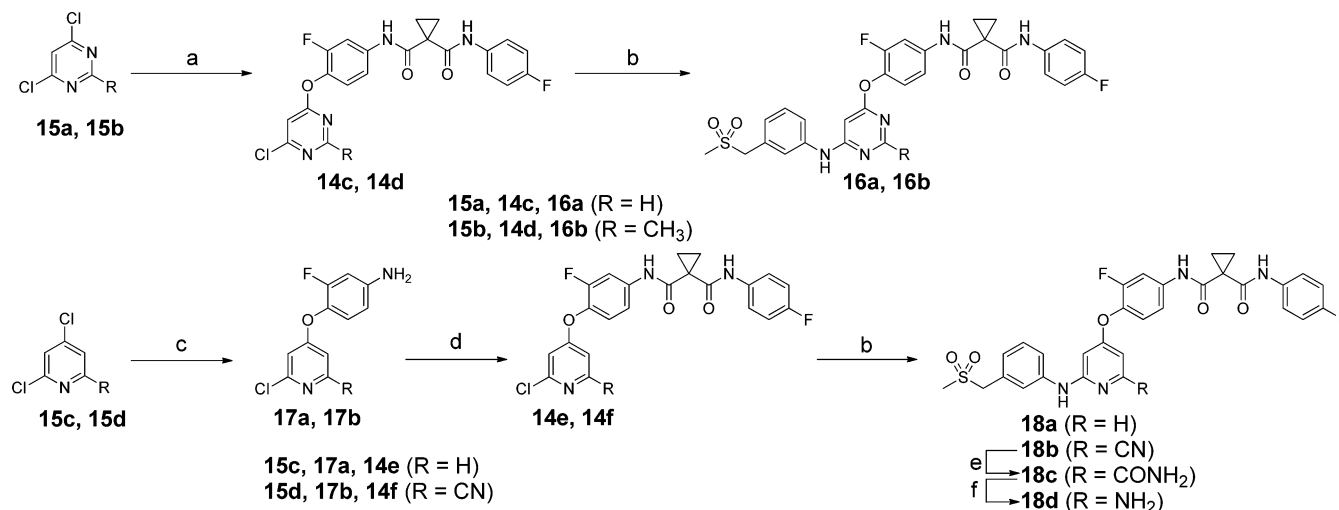
^aReagents and conditions: (a) **9b**, EDCl, DMF; (b) 2,4-dichloropyrimidine, K₂CO₃, DMF, 80 °C; (c) R'NH₂, Xantphos, Pd₂(dba)₃, Cs₂CO₃, 1,4-dioxane, 80 °C; (d) RNH₂, Et₃N, THF, 80 °C.

a series of compounds bearing an anilinyrimidine scaffold to explore their structure–activity relationships (SARs).

To achieve a rapid structure–activity relationship (SAR) exploration, two efficient synthetic routes were employed for preparation of the analogues. Scheme 1 illustrates the synthesis of **3a–f**, **3h–r**, **10b**, and **11**. Intermediates **7a–d** were prepared through an acid-catalyzed displacement of chloro compounds **5a** and **5b** with anilines **4a–4c** followed by a reduction reaction with iron powder. The condensation of **7a–d** with carboxylic acids **9a–n** afforded **3a–f**, **3h–r**, **10b**, and **11**. Schemes 2 and 3 outline the synthesis of analogues **3g**, **10a**, **10c–n**, **16a**, **16b**,

and **18a–d**. Buchwald–Hartwig reaction of chloro compounds **14a–f** with various arylamines provided **3g**, **10a**, **10c–l**, **16a**, **16b**, **18a**, and **18b**. However, analogues **10m** and **10n** were easily prepared from chloro compound **14b** with aliphatic amines through S_NAr displacement.

The compounds depicted in Tables 1–3 were assayed with the enzymatic activities against c-Met and VEGFR-2, using PF2341066¹⁵ and AP24534¹⁶ as comparison. The SARs of the analogues with the varied substitutions at A and B rings (Table 1) were first discussed. On the B ring, among the series of *para*-fluoro, bromo, chloro, methyl, trifluoromethyl substituted

Scheme 3. Synthesis of Compounds 16a, 16b, and 18a–d^a

^aReagents and conditions: (a) **13b**, K₂CO₃, DMF, 80 °C; (b) **4a**, Xantphos, Pd₂(dba)₃, Cs₂CO₃, 1,4-dioxane, 80 °C; (c) **12b**, KO^tBu, DMA, 80 °C; (d) **9b**, EDCI, DMF; (e) urea hydrogen peroxide, K₂CO₃, acetone/H₂O; (f) NaOH, NaClO, i-PrOH/H₂O.

Table 1. SAR of A and B Rings^a

Compd	R ¹	R ²	IC ₅₀ (nM) ^b	
			VEGFR-2	c-Met
3a	H	H	16.0 ± 4.0	8.8 ± 1.4
3b	H	<i>p</i> -F	14.0 ± 2.0	7.9 ± 0.4
3c	H	<i>p</i> -Cl	30.3 ± 4.2	32.5 ± 2.1
3d	H	<i>p</i> -Br	61.5 ± 8.9	66.4 ± 11.2
3e	H	<i>p</i> -CH ₃	54.0 ± 15.5	18.6 ± 4.6
3f	H	<i>p</i> -CF ₃	219.9 ± 70.3	184.0 ± 34.8
3g	2-F	<i>p</i> -F	4.0 ± 0.5	13.1 ± 1.6
3h	3-F	<i>p</i> -F	6.0 ± 1.0	6.7 ± 0.7
3i	3-F	<i>p</i> -Br	46.6 ± 5.9	70.6 ± 0.9
3j	3-F	<i>p</i> -OCH ₃	6.1 ± 1.6	337.6 ± 4.1
3k	3-F	<i>m</i> -OCH ₃	5.6 ± 0.1	683.1 ± 58.0
3l	3-F	<i>m</i> -CH ₃	42.7% @ 10 μM	81.9 ± 16.9
3m	3-F	H	12.7 ± 2.8	25.8 ± 7.7
3n	3-F	<i>m</i> -F	43.0 ± 7.0	155.1 ± 19.4
3o	3-F	<i>m</i> -Cl	9.8 ± 0.3	212.7 ± 9.7
3p	3-F	<i>m</i> -CF ₃	48.0 ± 8.0	234.3 ± 22.2
3q	3-F	<i>m</i> -CF ₃ , <i>p</i> -Cl	83.6 ± 0.9	791.9 ± 169.2
3r	3-F	<i>m</i> -CF ₃ , <i>p</i> -CN	44.5 ± 7.5	17.7% @ 10 μM

^aSee Supporting Information for a description of the assay conditions.
^bc-Met IC₅₀ of PF2341066 = 1.5 ± 0.3 nM; VEGFR-2 IC₅₀ of AP24534 = 4.3 ± 0.4 nM.

analogues (**3b–3f**), the activity of *para*-fluoro analogue **3b** was equipotent to that of **3a** on both c-Met and VEGFR-2, and the other substituents led to a substantial drop in potency on both c-Met and VEGFR-2. Substitution patterns on the B ring of **3h** revealed that c-Met was more sensitive to bulky substituents (**3i–k**, and **3o–r**). On the A ring, the 3-fluoro analogue **3h** displayed a better enzymatic potency than the 2-fluoro analogue **3g**, suggesting that 3-fluoro substitution is superior

to 2-fluoro substitution. X-ray crystallography of c-Met and **3h** (Figure 2) showed that the hydrophobic pocket where the A ring was accommodated did not tolerate bulky substituents; therefore, no further modification was carried out on the A ring.

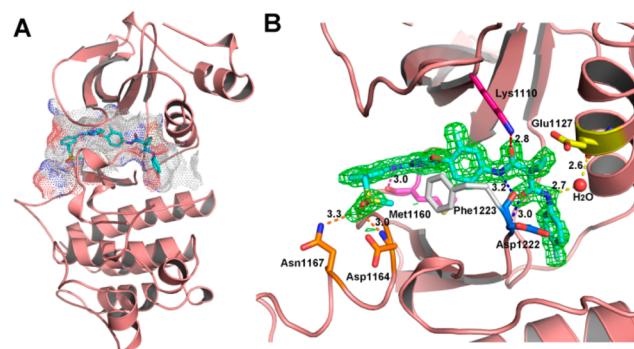
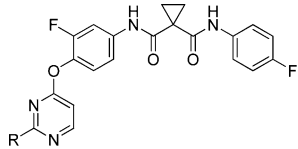
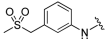
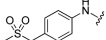
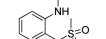
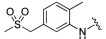
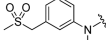
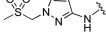
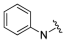
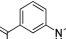
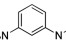
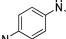
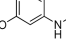
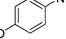
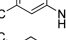
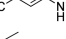
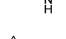
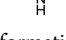


Figure 2. Cocystal structure of the compound **3h** in complex with the kinase domain of c-Met. The pdb code of the structure is 4MXC. (A) An overview of the complex structure. The molecular surface of **3h** buried into the kinase domain is represented by dots, and the compound is shown by sticks. (B) The hydrogen bond interactions (dash lines) as well as the π – π stacking interactions between **3h** and residues of c-Met.

With optimized A and B rings, we then investigated SARs on the 2-position of the pyrimidine of **3h** (Table 2). The *para*- and *ortho*-methylsulfonylmethyl analogues (**10a** and **10b**) displayed a lower potency than their *meta*-substituted counterpart **3h** in both VEGFR-2 and c-Met, indicating that *meta* substitution is preferred in this series of compounds. Compound **10e** was prepared to test the impact of removal of the methylsulfonylmethyl on its activity, and the result showed that this modification led to a sharp drop in potency on both c-Met and VEGFR-2. The drop in potency can be explained by the fact that the hydrogen bond between the methylsulfonyl oxygen and the backbone NH of Asp 1164 was essential for maintaining c-Met potency as was confirmed by the crystal structure of c-Met and **3h** (Figure 2B). To examine the role of NH in the anilinyrimidine moiety on the activity, we

Table 2. SAR of 2-Substituents on the Pyrimidine Ring^a


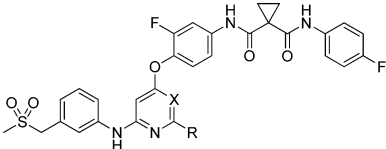
Compd	R	IC ₅₀ (nM) ^b	
		VEGFR-2	c-Met
3h		6.0±1.0	6.7±0.7
10a		52.0±13.0	23.4±1.2
10b		0.4%@10μM	36.9%@10μM
10c		24.5±3.6	149.9±24.0
11		42.7%@10μM	36.4%@10μM
10d		39.4%@10μM	44.8±4.9
10e		255.6±54.3	68.3±8.0
10f		181.0±13.0	51.7±1.1
10g		39.0%@10M	104.9±0.2
10h		21.5%@10μM	683.1±58.0
10i		230.0±4.0	113.8±27.1
10j		4394.0±563.0	52.6±3.0
10k		196.2±25.2	186.5±14.3
10l		2716.0±95.0	46.4%@10μM
10m		2468.5±47.7	248.9±54.5
10n		8.6%@10μM	168.9±17.8

^aSee Supporting Information for a description of the assay conditions.
^bc-Met IC₅₀ of PF2341066 = 1.5 ± 0.3 nM; VEGFR-2 IC₅₀ of AP24534 = 4.3 ± 0.4 nM.

prepared an *N*-methylated analogue **11**, but it was inactive against both c-Met and VEGFR-2. The loss of potency might be attributed to the loss of the hydrogen bond between NH and the backbone carbonyl oxygen of Met 1160 in the hinge region as shown in Figure 2B. Variations of substituents on the 2-position of pyrimidine were then examined. Much to our disappointment, substitution of *meta*-methylsulfonylmethylphenyl with methylsulfonylmethylpyrazolyl (**10d**), acetylphenyl (**10f**), nitrophenyl (**10g** and **10h**), trifluoromethylphenyl (**10k** and **10l**), and two alkyl (**10m** and **10n**) ended up with poor potencies in both c-Met and VEGFR-2. Therefore, we concluded that both the 3-methylsulfonylmethylaniline and *N*-(3-fluoro-phenyl)-*N'*-(4-fluoro-phenyl)cyclopropane-1,1-dicarboxamide moieties were crucial to the analogues for good potencies on both c-Met and VEGFR-2 as shown by the data in Tables 1 and 2.

As an extension of the 2,4-disubstituted pyrimidine chemotype, 4,6-disubstituted pyrimidine analogues and 2,4-disubsti-

tuted pyridine analogue were also explored (Table 3). The result showed that the 4,6-disubstituted pyrimidine analogues

Table 3. SAR of Pyrimidine Derivatives^a


Compd	R	X	IC ₅₀ (nM) ^b	
			VEGFR-2	c-Met
3h			6.0 ± 1.0	6.7 ± 0.7
16a	H	N	55.0 ± 13.0	21.7 ± 1.0
16b	CH ₃	N	37.4% @ 10 μM	924.0 ± 9.8
18a	H	CH	16.0 ± 3.0	3.8 ± 0.5
18b	CN	CH	0 @ 10 μM	805.8 ± 98.1
18c	CONH ₂	CH	3.1% @ 10 μM	211.1 ± 67.2
18d	NH ₂	CH	0 @ 10 μM	39.6% @ 10 μM

^aSee Supporting Information for a description of the assay conditions.
^bc-Met IC₅₀ of PF2341066 = 1.5 ± 0.3 nM; VEGFR-2 IC₅₀ of AP24534 = 4.3 ± 0.4 nM.

(**16a** and **16b**) exhibited decreased c-Met and VEGFR-2 potencies and that the pyridine analogue **18a** inhibited c-Met with an IC₅₀ value of 3.8 nM, a moderate improvement compared to **3h**. The crystal of **3h** in complex with the kinase domain of c-Met revealed that **3h** occupied the ATP-binding site as well as an adjacent pocket of the kinase domain and trapped the kinase in its inactive conformation (Figure 2A).¹⁷ The details of the hydrogen bonds were shown in Figure 2B. In particular, a π - π stacking interaction occurred between the phenyl ring of Phe1223 and the central fluorophenyl group of **3h**, which dislodges Phe1223 of the DFG motif from its activated conformation.¹⁷

The cellular assays commenced by testing the activities of the compounds with good enzymatic potencies (**3a**, **3b**, **3g**, **3h**, and **18a**) in MKN-45 gastric carcinoma cells. As shown in Table 4,

Table 4. Effects of Selected Analogues on Human Cancer Cell Proliferation^a

Compd	IC ₅₀ (μM)	
	MKN-45	EBC-1
3a	1.7 ± 0.04	
3b	1.3 ± 0.28	
3g	0.59 ± 0.04	0.72 ± 0.04
3h	1.1 ± 0.05	
18a	0.46 ± 0.001	0.33 ± 0.01

^aSee Supporting Information for a description of the assay conditions.

compounds **3g** and **18a** outperformed the other counterparts with IC₅₀ values of 0.59 and 0.46 μM, respectively. Moreover, **3g** and **18a** also demonstrated strong inhibition in EBC-1 (human nonsmall-cell lung cancer cell line) cells, though the assayed compounds suffered a decrease in enzyme-to-cell shift, which might be ascribed to the poor cellular penetration. In an immunoblot analysis of compound **3g** or **18a** treated EBC-1 cells, complete inhibition of c-Met phosphorylation was observed at a concentration of 0.5 μM (Figure 3). In addition, c-Met downstream signaling molecules (Erk 1/2 and AKT) were also significantly suppressed.¹⁸ These data suggest that

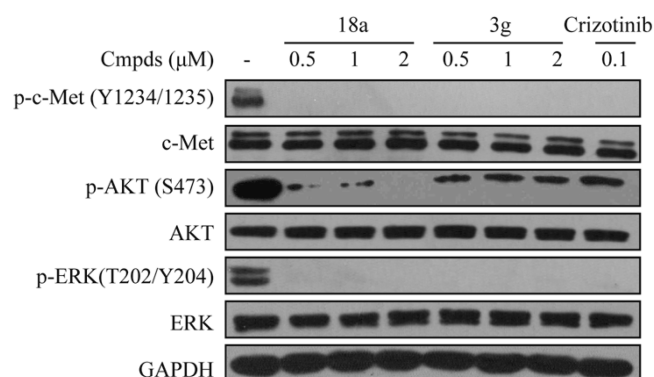


Figure 3. Inhibition of c-Met phosphorylation and related signaling pathways by compound **3g** and **18a** in EBC-1 cells.

inhibition of the phosphorylation of c-Met as well as the subsequent c-Met downstream signaling accounts for the antiproliferative potency of compounds **3g** and **18a**.

In summary, a series of novel and potent dual c-Met/VEGFR-2 tyrosine kinase inhibitors bearing an anilino-pyrimidine scaffold were designed and synthesized. Systematic SAR allowed us to identify several very potent c-Met/VEGFR-2 dual inhibitors. In addition to their enzymatic activities, the privileged compounds **3g** and **18a** demonstrated potent antiproliferative activities in MKN-45 and EBC-1 cancer cells, as well as inhibition of c-Met phosphorylation and its downstream signaling pathways in EBC-1 cells. Besides, the X-ray structure reveals that **3h** occupies the ATP-binding site as well as an adjacent pocket of c-Met kinase domain in an inactive conformation. Although none of our designed derivatives are better than cabozantinib at both enzymatic and cellular levels, this study has provided us with the clear SARs that are responsible for inhibition of c-Met/VEGFR-2 and will aid in the design of more potent dual c-Met/VEGFR-2 inhibitors.

■ ASSOCIATED CONTENT

Supporting Information

Synthetic procedures and analytical data for compounds reported in this letter, procedures for enzymatic and cellular assays, and procedures for X-ray cococrystallization. This material is available free of charge via the Internet at <http://pubs.acs.org>.

■ AUTHOR INFORMATION

Corresponding Authors

*(W.D.) E-mail: whduan@simm.ac.cn. Phone: +86-21-50806032.

*(M.G.) E-mail: mygeng@simm.ac.cn.

*(Y.X.) E-mail: yxcu@simm.ac.cn.

Author Contributions

†(Z.Z., J.A., and Q.L.) These authors contributed equally to this work.

Funding

We thank the National Natural Science Foundation of China (no. 81273365 and 81102461), Major Projects in National Science and Technology of China (no. 2010ZX09401-401, 2012ZX09103101-024, and 2012ZX09301001-007), National Program on Key Basic Research Project of China (2012CB910704), and the "100 Talents Project" of CAS (to Y.X.) for their financial support.

Notes

The authors declare no competing financial interest.

■ REFERENCES

- (1) Comoglio, P. M.; Giordano, S.; Trusolino, L. Drug development of MET inhibitors: targeting oncogene addiction and expedience. *Nat. Rev. Drug Discovery* **2008**, *7*, 504–516.
- (2) Birchmeier, C.; Birchmeier, W.; Gherardi, E.; VandeWoude, G. F. Met, metastasis, motility and more. *Nat. Rev. Mol. Cell Biol.* **2003**, *4*, 915–925.
- (3) Cheng, H.-L.; Trink, B.; Tzai, T.-S.; Liu, H.-S.; Chan, S.-H.; Ho, C.-L.; Sidransky, D.; Chow, N.-H. Overexpression of c-MET as a prognostic indicator for transitional cell carcinoma of the urinary bladder: a comparison with p53 nuclear accumulation. *J. Clin. Oncol.* **2002**, *20*, 1544–1550.
- (4) Otsuka, T.; Takayama, H.; Sharp, R.; Celli, G.; LaRochelle, W. J.; Bottaro, D. P.; Ellmore, N.; Vieira, W.; Owens, J. W.; Anver, M.; Merlino, G. c-Met autocrine activation induces development of malignant melanoma and acquisition of the metastatic phenotype. *Cancer Res.* **1998**, *58*, 5157–5167.
- (5) Drebber, U.; Baldus, S. E.; Nolden, B.; Grass, G.; Bollschweiler, E.; Dienes, H. P.; Hölscher, A. H.; Mönig, S. P. Overexpression of c-MET as a prognostic indicator for gastric carcinoma compared to p53 and p21 nuclear accumulation. *Oncol. Rep.* **2008**, *19*, 1477–1483.
- (6) Folkman, J. Role of angiogenesis in tumor growth and metastasis. *Semin. Oncol.* **2002**, *29* (6 Suppl. 16), 15–18.
- (7) Ferrara, N. Role of vascular endothelial growth factor in the regulation of angiogenesis. *Kidney Int.* **1999**, *56*, 794–814.
- (8) Ferrara, N.; Gerber, H. P.; LeCouter, J. The biology of VEGF and its receptors. *Nat. Med.* **2003**, *9*, 669–676.
- (9) Mannion, M.; Raeppl, S.; Claridge, S.; Zhou, N.; Saavedra, O.; Isakovic, L.; Zhan, L.; Gaudette, F.; Raeppl, F.; Déziel, R.; Beaulieu, N.; Nguyen, H.; Chute, I.; Beaulieu, C.; Dupont, I.; Robert, M.-F.; Lefebvre, S.; Dubay, M.; Rahil, J.; Wang, J.; Ste-Croix, H.; Macleod, A. R.; Besterman, J. M.; Vaisburg, A. N-(4-(6,7-Disubstituted-quinolin-4-yloxy)-3-fluorophenyl)-2-oxo-3-phenylimidazolidine-1-carboxamides: A novel series of dual c-Met/VEGFR2 receptor tyrosine kinase inhibitors. *Bioorg. Med. Chem. Lett.* **2009**, *19*, 6552–6556.
- (10) Claridge, S.; Raeppl, F.; Granger, M.-C.; Bernstein, N.; Saavedra, O.; Zhan, L.; Llewellyn, D.; Wahhab, A.; Deziel, R.; Rahil, J.; Beaulieu, N.; Nguyen, H.; Dupont, I.; Barsalou, A.; Beaulieu, C.; Chute, I.; Gravel, S.; Robert, M.-F.; Lefebvre, S.; Dubay, M.; Pascal, R.; Gillespie, J.; Jin, Z.; Wang, J.; Besterman, J. M.; MacLeod, A. R.; Vaisburg, A. Discovery of a novel and potent series of thieno[3,2-*b*]pyridine-based inhibitors of c-Met and VEGFR2 tyrosine kinases. *Bioorg. Med. Chem. Lett.* **2008**, *18*, 2793–2798.
- (11) Bilanges, B.; Torbett, N.; Vanhaesebroeck, B. Killing two kinase families with one stone. *Nat. Chem. Biol.* **2008**, *4*, 648–649.
- (12) Yakes, F. M.; Chen, J.; Tan, J.; Yamaguchi, K.; Shi, Y.; Yu, P.; Qian, F.; Chu, F.; Bentzien, F.; Cancelli, B.; Orf, J.; You, A.; Laird, A. D.; Engst, S.; Lee, L.; Lesch, J.; Chou, Y.-C.; Joly, A. H. Cabozantinib (XL184), a novel MET and VEGFR2 inhibitor, simultaneously suppresses metastasis, angiogenesis, and tumor growth. *Mol. Cancer Ther.* **2011**, *10*, 2298–2308.
- (13) Kurzrock, R.; Sherman, S. I.; Ball, D. W.; Forastiere, A. A.; Cohen, R. B.; Mehra, R.; Pfister, D. G.; Cohen, E. E. W.; Janisch, L.; Nauling, F.; Hong, D. S.; Ng, C. S.; Ye, L.; Gagel, R. F.; Frye, J.; Müller, T.; Ratain, M. J.; Salgia, R. Activity of XL184 (Cabozantinib), an oral tyrosine kinase inhibitor, in patients with medullary thyroid cancer. *J. Clin. Oncol.* **2011**, *29*, 2660–2666.
- (14) Sammond, D. M.; Nailor, K. E.; Veal, J. M.; Nolte, R. T.; Wang, L.; Knick, V. B.; Rudolph, S. K.; Truesdale, A. T.; Nartey, E. N.; Stafford, J. A.; Kumar, R.; Cheung, M. Discovery of a novel and potent series of dianilino-pyrimidineurea and urea isostere inhibitors of VEGFR2 tyrosine kinase. *Bioorg. Med. Chem. Lett.* **2005**, *15*, 3519–3523.
- (15) Cui, J. J.; Tran-Dubé, M.; Shen, H.; Nambu, M.; Kung, P. P.; Pairish, M.; Jia, L.; Meng, J.; Funk, L.; Botrous, I.; McTigue, M.; Grodsky, N.; Ryan, K.; Padriquet, E.; Alton, G.; Timofeevski, S.;

Yamazaki, S.; Li, Q.; Zou, H.; Christensen, J.; Mroczkowski, B.; Bender, S.; Kania, R. S.; Edwards, M. P. Structure based drug design of crizotinib (PF-02341066), a potent and selective dual inhibitor of mesenchymal-epithelial transition factor (c-MET) kinase and anaplastic lymphoma kinase. *J. Med. Chem.* **2011**, *54*, 6342–6363.

(16) O'Hare, T.; Shakespeare, W. C.; Zhu, X.; Eide, C. A.; Rivera, V. M.; Wang, F.; Adrian, L. T.; Zhou, T.; Huang, W. S.; Xu, Q.; Metcalf, C. A., III; Tyner, J. W.; Loriaux, M. M.; Corbin, A. S.; Wardwell, S.; Ning, Y.; Keats, J. A.; Wang, Y.; Sundaramoorthi, R.; Thomas, M.; Zhou, D.; Snodgrass, J.; Commodore, L.; Sawyer, T. K.; Dalgarno, D. C.; Deininger, M. W.; Druker, B. J.; Clackson, T. AP24534, a pan-BCR-ABL inhibitor for chronic myeloid leukemia, potently inhibits the T315I mutant and overcomes mutation-based resistance. *Cancer Cell* **2009**, *16*, 401–412.

(17) Liu, Y.; Gray, N. S. Rational design of inhibitors that bind to inactive kinase conformations. *Nat. Chem. Biol.* **2006**, *2*, 358–364.

(18) Bertotti, A.; Burbridge, M. F.; Gastaldi, S.; Galimi, F.; Torti, D.; Medico, E.; Giordano, S.; Corso, S.; Rolland-Valognes, G.; Lockhart, B. P.; Hickman, J. A.; Comoglio, P. M.; Trusolino, L. Only a subset of Met-activated pathways are required to sustain oncogene addiction. *Sci. Signaling* **2009**, *2*, ra80.